GIS Integration Based on Supervised Learning Classification of Land Cover Change and Its Impact on Peak Discharge in North Bandung Area

Muhammad Rifqi Naufaldi[1*], Rina Marina Masri[1]
[1]Civil Engineering Study Program, Indonesia University of Education
*Corresponding Author: Muhammad Rifqi Naufaldi. Email: Mr0230005@gmail.com

Abstract

Rainfall during the rainy season should be supported by available water catchment area. However, rainfall that falls is often unable to be fully contained, resulting in flooding. This can be caused by ecosystem disturbances such as forest degradation and other reduction in vegetation areas, which will reduce the land's ability to absorb water because groundwater bound by vegetation is also reduced. In addition, the imbalance between land demand and supply often results in urban expansion to suburban areas, reducing available open land areas, as occurred in the North Bandung Area (NBA) in Bandung, West Java. This study was conducted to determine changes in land cover in the North Bandung Area against changes in peak discharge in a case study of the Cidurian sub-watershed. The method used was supervised learning classification to analyze land cover and land changes, and the Soil Conservation Services Curve Number (SCS-CN) method to determine the magnitude of the peak discharge by considering land cover parameters, soil type, and rainfall. The analysis was conducted throughout 2013-2023 with the results of changes in peak discharge of between 2013 and 2023 of 8.3 m^3/s.

Keywords : Supervised learning, multi spectral imaging, land cover change, SCS-CN, peak discharge

1. INTRODUCTION .

1.1. Background

. As the rainy season approaches, rainfall intensity tends to be higher and the duration longer than usual. This high rainfall should be supported by water catchment areas, which are prioritized for water catchment. However, in reality, rainfall is often unable to be fully contained. Ecosystem disturbances, such as forest and vegetation degradation, reduce the land's ability to absorb water because the groundwater bound by vegetation is also reduced. As a result, uncontrolled rainwater runoff flows to lower elevations. Furthermore, disturbed river basins and poor watershed management contribute to problems that can lead to flooding during the rainy season.

Forest cover is one factor in managing water runoff from heavy rainfall. Forest cover is part of the limited availability of space and land, so proper land use management and planning are necessary to maintain its availability. However, the imbalance between demand and supply of land often results in urban expansion to the outskirts, thus reducing the available open land area, as is the case in the North Bandung Area (NBA) in Bandung.

To study how land use changes occur, appropriate and suitable methods are needed to analyze spatial data on land cover changes over time. This can be achieved through the application of Geographic Information Systems (GIS). Furthermore, in the current era of the 4-th Industrial Revolution, which combines human and machine learning, GIS can utilize artificial intelligence through the concept of supervised learning. However, the application of GIS through supervised learning is a new concept that has not been widely studied in Indonesia, requiring further study.

Based on this problem description, this research will examine the impact of land use change on peak discharge of flood in the North Bandung area. The research location is the Cidurian sub-watershed, which originates in the North Bandung area and flows downstream in Bandung City.

1.2. Research and Limitations

The research problem addressed requires methodological limitations. The author limits this research to the following:

a. Massive land use conversion in the NBA area, resulting in ecological damage in the area.
b. Increased rainwater runoff from the NBA area to the underlying area due to a lack of water absorption due to environmental damage.
c. Frequent flooding, especially during the rainy season, in the districts of Bandung City.

1.3. Problems Formulation

The problems raised and resolved through this scientific paper are as follows:

a. How did land cover change occurred in the Cidurian sub-watershed between 2013 and 2023?
b. How did runoff from the Cidurian sub-watershed changed based on changes in the runoff curve number (CN) of the sub-watershed's land use between 2013 and 2023?
c. How much the peak flood discharge in the Cidurian sub-watershed based on the land use changes that occurred from 2013 to 2023?

1.4 Research Objectives

This research was conducted with the following objectives:

a. To determine the magnitude of land use changes occurring in the Cidurian sub-watershed between 2013 and 2023.
b. To calculate the magnitude of changes in the runoff curve number (CN) and other parameters of the Cidurian sub-watershed based on land use changes in the Cidurian sub-watershed between 2013 and 2023.
c. To calculate the peak flood discharge of the Cidurian sub-watershed based on land use changes in the Cidurian sub-watershed between 2013 and 2023.

2. METHOD

2.1. Land Cover Analysis

2.1.1. Case Study Area

Bandung City is part of the Bandung Basin (Greater Bandung), an area consisting of Bandung City, Cimahi City, Bandung Regency, West Bandung Regency, and part of Sumedang Regency. The Bandung Basin itself originates from the surrounding mountains. To the north, the Bandung Basin is bordered by Tunggul Hill, Tangkubanparahu, and Burangrang. To the east is Mandalawangi. To the south, the Bandung Basin is bordered by mountains, including Patuha, Tilu, Malabar, Sanggar, and Guntur. (Sunandar, 2024)

The Bandung Basin directly touches the Upper Citarum Watershed, with its sub-watersheds: Cimahi, Cibeureum, Citepus, Cikapundung, Cicadas, Cidurian, Cipamokolan, Cikeruh, Citarik, Cisangkuy, Ciboleran, and Ciwidey. These sub-watersheds are located in four cities and regencies within the Bandung region: Bandung City, Bandung Regency, West Bandung Regency, and Cimahi City.

The case study location is in the Cidurian sub-watershed, which originates in Cimenyan District in the North Bandung region. The research area then extends to Cibeunying District, Kiaracondong District, Antapani District, Buahbatu District, and finally to the outlet in Rancasari District.

.

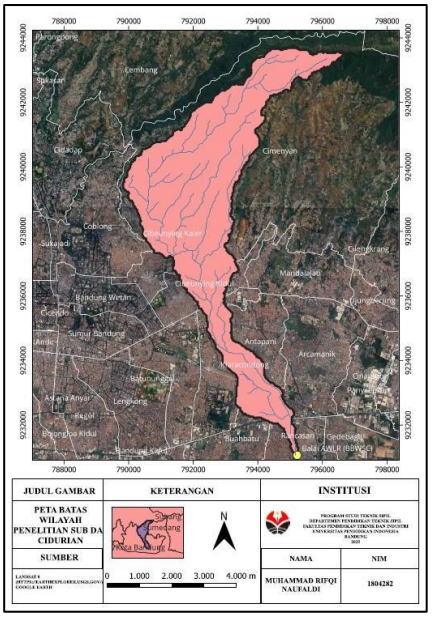

Fig. 1. Research area boundary map of Cidurian Sub-watershed

2.1.2. Multispectral Land Cover Classification

Land cover/land use classification is an effort to group various types of land cover/land use into a similarity according to a certain system. (Sitorus, Leonataris, & Panuju, 2012). Land cover/land use classification is used as a guideline or reference in the process of interpreting remote sensing imagery for the purpose of land cover/land use mapping. Many land cover/land use classification systems have been developed, which are motivated by certain interests or at certain times.

According to Danoedoro (2012) (in Wulansari, 2016), multispectral classification is a method designed to derive thematic information by grouping phenomena based on specific criteria. It is essentially assumed that each object can be distinguished from other objects based on its spectral value, with each object tending to exhibit a specific spectral response pattern.

Multispectral images are the output of multispectral remote sensing. According to Rehder (in Yusuf, 2017), multispectral remote sensing is remote sensing using more than one spectrum, all of which are captured simultaneously and from the same location and altitude. The sensors are either multi-lens cameras or single cameras with multiple lenses. Multispectral photos use various spectral groups, namely from a wavelength of 0.4 µm to 1.1 µm, which consist of groups of spectrum channels, namely: (a) blue channel (0.4 µm-0.5 µm), (b) green channel (0.5 µm- 0.6 µm), (c) red channel (0.6 µm -0.7 µm), and (d) infrared channel (0.8 µm- 2.3 µm).

2.1.3. Supervised Classification

In supervised classification, we train a computer to distinguish between land cover objects based on multispectral satellite imagery that has been composited into false colors. False color is an image processing technique that produces colors that differ from the original. The false color composite image is arranged to further enhance the contrast in differentiating object types within the study area.

2.1.4. Accuracy Assessment

Accuracy assessment is essentially conducted to determine the quality of information obtained from remote sensing data. This assessment can be qualitative or quantitative. Qualitative assessments typically involve a quick comparison to determine whether the remote sensing data or map looks right and corresponds to what is actually happening on the ground. Quantitative assessments attempt to identify and quantify errors in remote sensing maps. In supervised classification accuracy testing, the resulting map data is compared with reference data or actual field data that serves as validation for the map. (Knudby, 2021).

2.2. Hydrologic Analysis

2.2.1. Soil Consevation Services (SCS) Curve Number

The Soil Conservation Service Curve Number (SCS-CN) is a model developed by the Natural Resources Conservation Service (NRCS CN) to estimate the amount of runoff in a river basin or sub-basin. The SCS-CN

method is simple, predictable, and stable. However, over long periods of use, the infiltration value will approach zero, rather than remain constant. (USACE, 2025)

The parameters required to calculate loss using this method are the curve number, derived from land cover data, soil classification based on hydrology soil group (HSG), and rainfall (Delani & Dasanto, 2016). The curve number (CN) ranges from 30 to 100. A curve number of 30 represents a soil area with a high infiltration capacity, while a curve number of 100 (representing a body of water) indicates that all rainfall flows as direct runoff. (USACE, 2025) In addition to the curve number, another parameter taken into account is imperviousness, which refers to the extent of the area that is impermeable or unable to absorb water. (Tisnasuci, Sukmono, & Hadi, 2021) The following is a table of CN values based on land cover and soil classification:

Table 1: Determination of CN Value Based on Land Cover

Land cover	**% Impervious**	**CN value 'Hydrologic Soil Group"**			
		A	*B*	*C*	*D*
Water	100	100	100	100	100
Forest	-	30	55	70	77
Open space	-	49	69	79	84
Developed area	65	77	85	90	92
Mixed scrub	-	43	65	76	82
Agriculture	-	61	70	77	80
Rice field	-	63	75	83	87

(Tisnasuci, Sukmono, & Hadi, 2021)

2.2.2. SCS Unit Hydrograph

The SCS synthetic unit hydrograph method was developed in the United States by Victor Mocus of The Soil Conservation Service (SCS) in 1972. The SCS unit hydrograph method uses a dimensionless curved unit hydrograph to channel rainfall runoff to the watershed outlet. (USACE, 2025). In this hydrograph, the discharge ordinate is the ratio between discharge (q) and peak discharge (qp) and the time abscissa is the ratio between time (t) and peak time (tp), where the rise time (Tp) can be expressed as a fraction of the peak time tp and the effective rainfall duration tr. (Sari, Pranoto, & Suryan, 2020).

Based on the analysis of river watershed characteristics, several parameters can be identified that will be used to determine the shape of the SCS unit hydrograph. The details of these parameters are as follows: (Sari, Pranoto, & Suryan, 2020)

a. Watershed Physical Characteristics Data
   Data required to calculate the SCS unit hydrograph include watershed area, river slope, and river length.
b. Transformation Parameters
   Determining transformation parameters is used to calculate the direct flow of rainwater runoff. Transformation parameters include Time Lag (TL) and Time of Concentration (Tc). Time of Concentration is the time required for rainwater to flow from the furthest point in a watershed to the outlet point. Kent et al., 2010 formulated the empirical calculation of time concentration and lag time as follows:

$$T_C = \frac{l^{0,8}.\,(S+1)^{0,7}}{1{,}140Y^{0,5}} \quad (1)$$

$$\text{Lag} = 0{,}6T_c \quad (2)$$

Where:
L = Lag, (hours)
Tc = Time of concentration, (hours)
L = Stream length, (ft)
Y = Average watershed slope (%)
S = Maximum potential impermeability (in), where

$$S = \frac{1000}{CN} - 10 \quad (3)$$

3. Results and Discussion

3.1. Land cover change analyses

In this study, land cover maps were created using QGIS LTR 3.34 software. To create supervised learning-based land cover maps in QGIS, the Semi-Automatic Classification Plug-in (SCP) Version 7.10 plug-in must be downloaded and installed on the computer prior to analysis. This plug-in can assist in supervised land cover

classification analysis, integrating the steps from pre-processing, processing, and post-processing of land cover maps (Congedo, 2021). The land cover classification process, conducted by a machine learning algorithm (AI), will refer to various ROI samples and spectral signatures created within the plug-in.

3.1.1. Land Cover based on Supervised Classification

The results of the land cover classification are raster data output with coloring based on predetermined land classes. An example of the raster output is shown in the 2013 Land Cover Map of the Cidurian sub-watershed below:

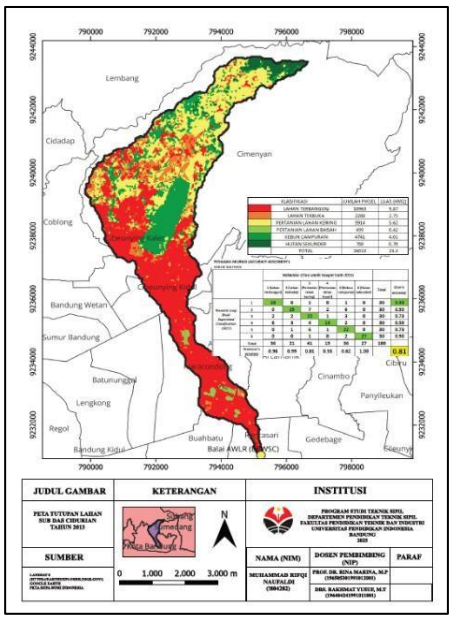

Fig. 2. Land cover map of Cidurian Sub-watershed in 2013

3.1.2. Accuracy Assessment

In this study, to test accuracy, the classified map data from each year was then compared with historical imagery reference data from Google Earth satellite imagery, which served as validation for the map.

Accuracy testing can be performed using the Accuracy Assessment for Thematic Maps (AcATaMa) plug-in in QGIS (Llano, 2024). The analysis results are displayed as a confusion matrix (error matrix). The following is an example of a confusion matrix obtained from the accuracy test on the 2013 Cidurian Sub-Watershed Land Cover Map:

Table 2: Confusion Matrix of Land Cover Map of Cidurian Sub-watershed in 2013

		***Validation* (Google Earth Satellite image2013)**							
		1 (Built-up)	**2 (Open space)**	**3 (Agriculture)**	**4 (rice field)**	**5 (mixed shrubs)**	**6 (secondary forest)**	**Total**	***User's accuracy***
Thematic map (Supervised Classification 2013)	**1**	**28**	**0**	**1**	**0**	**1**	**0**	**30**	**0.93**
	2	**0**	**15**	**7**	**2**	**6**	**0**	**30**	**0.50**
	3	**2**	**2**	**22**	**1**	**3**	**0**	**30**	**0.73**
	4	**6**	**3**	**4**	**15**	**2**	**0**	**30**	**0.50**
	5	**0**	**1**	**6**	**1**	**22**	**0**	**30**	**0.73**
	6	**0**	**0**	**1**	**0**	**2**	**27**	**30**	**0.90**
	Total	**36**	**21**	**41**	**19**	**36**	**27**	**180**	
	Producer's accuracy	**0.96**	**0.62**	**0.72**	**0.21**	**0.70**	**1.00**		**0.81**

Overall accuracy is the accuracy used to determine the suitability of a land cover map. Based on Olson's (2008) findings regarding the criteria for creating land cover maps, the minimum overall accuracy requirement for a land cover map to be considered suitable for use is 0.80 or 80%.

3.1.3. Land Cover Change

In this study, based on the results of the creation of a supervised classification land cover map raster, accuracy testing of validation data, and various iterations that have been carried out from 2013-2023, the area of each land class and the accuracy of the map in each year are obtained, which are presented in the following table:

Table 2: Land class area and overall accuracy of the Cidurian sub-watershed land cover map for 2013-2023

Year (n)	**2013**	**2014**	**2015**	**2016**	**2017**	**2018**	**2019**	**2020**	**2021**	**2022**	**2023**
Built-up (km^2)	9.87	9.93	10.01	10.09	10.13	10.18	10.30	10.44	10.64	10.84	11.00
Open space (km^2)	2.75	2.87	2.83	2.67	2.43	2.77	2.60	2.26	2.06	1.96	1.86
Agriculture (km^2)	5.62	5.56	5.02	5.32	5.22	5.05	5.25	5.09	5.32	5.57	5.34
Rice field (km^2)	0.42	0.18	0.39	0.24	0.45	0.22	0.08	0.26	0.45	0.35	0.27
Mixed shrubs (km^2)	4.01	4.17	4.46	4.43	4.46	4.51	4.43	4.57	4.27	4.00	4.27
Secondary forest (km^2)	0.76	0.72	0.72	0.70	0.73	0.70	0.77	0.81	0.69	0.71	0.68
Overral accuracy (%)	**80.65**	**87.71**	**84.39**	**80.95**	**80.08**	**80.21**	**81.03**	**86.09**	**84.78**	**84.02**	**83.43**

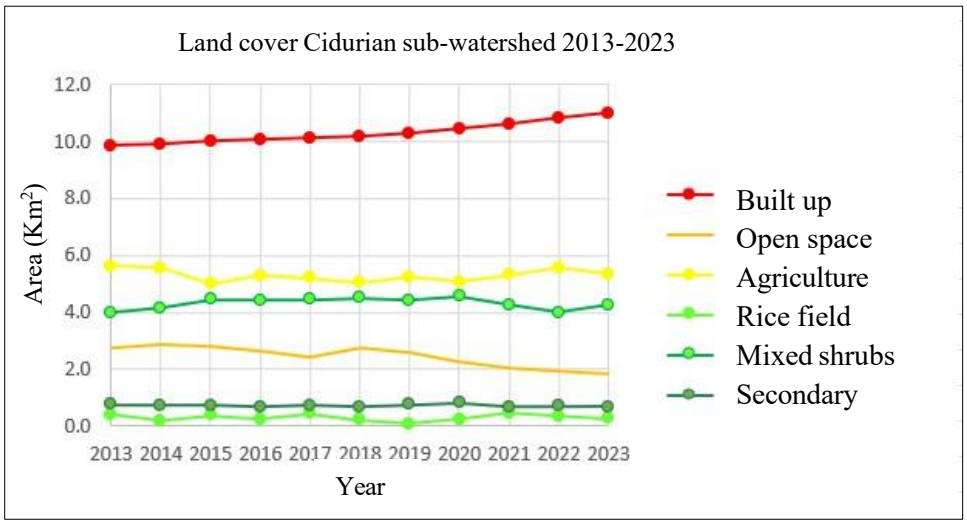

Fig. 3. Land cover of Cidurian Sub-watershed from 2013-2023

Based on the analysis results that can be seen in the graph and table, the overall raster accuracy value has exceeded 80% in each year, so that the entire land cover map can be said to be suitable for use in the next stages of analysis.

3.2. Hydrologic analyses

3.2.1. Loss parameters (Curve Number)

The Curve Number value distribution map was created using the QGIS program, with a dedicated tool extension for analyzing Curve Number values, the Curve Number Generator plug-in (Siddique, 2020). In this plug-in, the input data for the Curve Number map are a land cover map, a Hydrologic Soil Group (HSG) soil type map, and a Curve Number Tr-55 table.

The following is an example of the analysis output which is a Curve Number Value Distribution Map for the Cidurian sub-DAS in 2013.

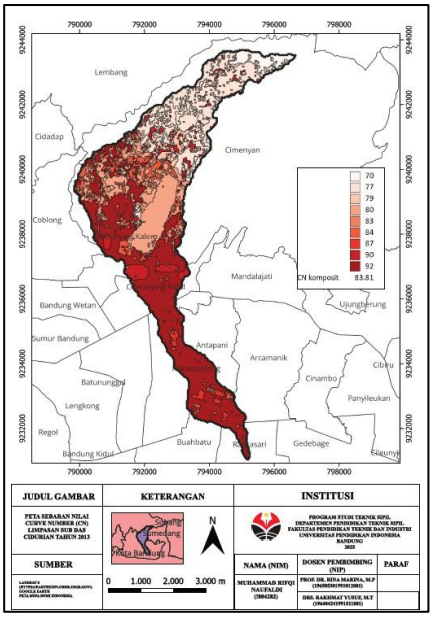

Fig. 4. Curve Number Map of Cidurian Sub-watershed in 2013

Based on the results of the creation of a Curve Number value distribution map from 2013-2023, the average CN value can be obtained based on statistical calculations in the QGIS program, and in this study, the Area-Weighted-Average plug-in was used in QGIS to calculate the average value statistics (Siddiqui, 2021).

Table 3. The average value of CN of the Cidurian sub-watershed in 2013-2023

Year		Composite Curve Number (CN)					
	Sub basin	1	2	3	4	5	Total area composite
2013		79.228	80.266	81.329	83.242	87.703	82.02
2014		79.258	80.353	81.438	83.344	87.723	82.06
2015		79.276	80.5	81.603	83.348	87.751	82.11
2016		79.415	80.557	81.622	83.349	87.758	82.19
2017		79.418	80.651	81.928	83.395	87.792	82.24
2018		79.497	80.66	81.965	83.45	87.81	82.29
2019		79.522	80.775	82.01	83.506	87.859	82.33
2020		79.57	80.868	82.026	83.593	87.917	82.39
2021		79.682	80.909	82.277	83.625	87.991	82.49
2022		79.742	81.08	82.503	83.64	88.002	82.56
2023		79.886	81.62	82.557	83.695	88.023	82.71

3.2.2. Transform parameter

The transformation parameters are used to calculate the direct flow of rainwater runoff. The results of the Tc and Lag time parameter calculations are shown in the following table:

Table 4. Results of Tc and Lag time parameter calculations in the Cidurian sub-watershed

Year	CN	S (inch)	Y	l	Tc (jam)	Lag time (hour)	lag time (minute)
2013	83.808	1.932	16.960	67969.523	3.321	1.993	119.550
2014	83.821	1.930	16.960	67969.523	3.319	1.992	119.497
2015	83.890	1.920	16.960	67969.523	3.312	1.987	119.216
2016	83.897	1.919	16.960	67969.523	3.311	1.986	119.190
2017	83.916	1.917	16.960	67969.523	3.309	1.985	119.114
2018	83.929	1.915	16.960	67969.523	3.307	1.984	119.060
2019	83.959	1.911	16.960	67969.523	3.304	1.982	118.940
2020	83.987	1.907	16.960	67969.523	3.301	1.980	118.826
2021	84.114	1.889	16.960	67969.523	3.286	1.972	118.308
2022	84.194	1.877	16.960	67969.523	3.277	1.966	117.987
2023	84.254	1.869	16.960	67969.523	3.271	1.962	117.744

3.3. Peak Discharge Analysis

3.3.1. Rainfall Design

The Rainfall Design Analysis includes various calculation stages, including regional rainfall calculations, data distribution calculations, frequency distribution calculations, rainfall data suitability test calculations, and hourly rainfall distribution pattern calculations.

The selection of rainfall distribution methods is carried out by comparing the distribution coefficients of the methods to be used. The results of the distribution selection calculations in this study can be seen in the following table:

Table 5. Calculation results for selecting the rain distribution method

No.	Distribution	Requirements	Calculation result	Requirement result
1.	Normal	$C_s \approx 0$	Cs = 2,124	Not eligible
		$C_k \approx 3$	Ck = 9,150	
2.	Log Normal	$C_s \approx C_v^3 + 3C_v$	Cs = 1,131 $C_v^3 + 3C_v = (0{,}069)^3 + 3(0{,}069) = 0{,}208$	Not eligible
		$C_k \approx C_v^8 + 6C_v^6 + 15C_v^4 + 16C_v^2 + 3$	Ck = 6,314, $C_v^8 + 6C_v^6 + 15C_v^4 + 16C_v^2 + 3 = (0{,}069)^8 + 6\ (0{,}069)^6 + 15(0{,}069)^4 + 16(0{,}069)^3 + 3 = 3{,}077$	
3.	Gumbel	$C_s \approx 3C_v + C_v^3 = 3$	$3\ Cv + Cv^3 = 3(0{,}352) + (0{,}352)^3 = 1{,}180$	Not eligible
		$C_k \approx 5{,}4$	Ck = 9,07	
4	Log Pearson III	Apart from the above values	Cs = 1,131 Ck = 6,314	Eligible

Based on the calculation results, the type of distribution method that meets the requirements is Log Pearson III, so this method was chosen as the calculation method in the frequency distribution analysis. Based on the distribution of log pearson III rainfall, the design rainfall with a return period of Tr = 100 years is 192 mm. Calculation of rain intensity and rain distribution patterns is carried out using the Mononobe method to calculate rain intensity,

Table 6. Rain design distribution

Td (hour).	P
1	14
2	20
3	58
4	35
5	25
6	17
	192

3.3.2. Peak Discharge Calculations

Based on the design rainfall analysis and previously calibrated parameters, the peak flood discharge can then be calculated for each observation year through the HEC-HMS simulation run. In this study, the simulation results, in the form of the Q100 peak flood discharge hydrograph output, are displayed as follows:'

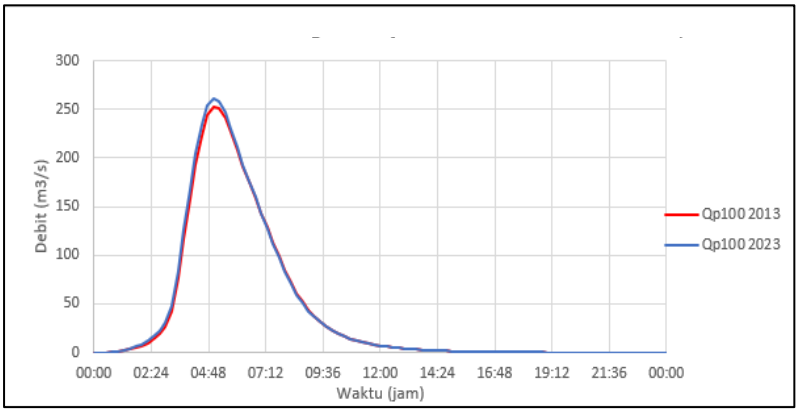

Fig. 5. Unit hydograph based on Q_{100} of Cidurian Sub-watershed 2013 & 2023

Table 7. Q100 peak discharge simulation results for 2013-2023

Year	Q100
2013	196.4
2014	196.9
2015	197.3
2016	198.1
2017	198.5
2018	199.3
2019	200
2020	201.6
2021	202
2022	202.9
2023	204.7

4. Conclusions

Based on the results of the analysis, it can be concluded as follows:

a. Land use change analysis was conducted on six land cover classes, namely built-up land, open land, dryland agriculture (fields), wetland agriculture (rice fields), mixed gardens, and secondary forests. Based on the analysis results, the highest land use change occurred in the change from open land to built-up land, with a change of 0.86 km2 during the 2013-2023 period, followed by the change from open land to dryland agriculture (fields) of 0.81 km2. The land use change with the least area occurred in the secondary forest land class with a reduction of 0.08 km2 over the 11-year period. The entire land cover map has an overall accuracy of >0.8, making it suitable for use in subsequent analyses.

b. Based on the analysis results, the value of the curve number during the period 2013-2023, the composite CN value of the Cidurian sub-watershed experienced a slight increase from 82.02 in 2013 to 82.71 in 2023, with an average increase of 0.06 each year. Meanwhile, based on the analysis results of the impervious value, during the period 2013-2023 the average impervious value of the Cidurian sub-watershed experienced an increase from 26.45% in 2013 to 29.87% in 2023 with an average increase of 0.31% each year.

c. Based on the results of the flood discharge analysis, the peak discharge in the Cidurian sub-watershed experienced little change during the period 2013-2023. At the peak flood discharge with a 100-year return period (Qp100), the discharge changed from 196.9 m3/second in 2013 to 204.7 m3/second in 2023 with an average change of 0.75 m3/second each year.

ACKNOWLEDGMENT

The author expresses sincere gratitude to Prof. Dr. Rina Marina Masri, M.P, as the supervisor, the Civil Engineering Department at Indonesia University of Education, and BBWS Citarum for granting acces and data for this research.

REFERENCES

Congedo L. Semi-Automatic Classification Plugin: A Python tool for the download and processing of remote sensing images in QGIS. Journal of Open Source Software, 6(64), 3172. https://doi.org/10.21105/joss.03172. 2021.

Delani OM, Dasanto DB. Perbandingan Hidograf Banjir Menggunakan Beberapa Metode Perhitungan Curah Hujan Efektif. Jurnal Sumber Daya Air. 2016;: 187-198.

Kent KM, Woodward DE, Hoeft CC, Huimpal A, Cerrelli G, Jacobsen S, et al. Chapter 15 : Time of concentration. In Hydrology national Engineering Handbook.: United States Department of Agriculture; 2010.

Knudby A. Remote sensing. Open Library. [Online].; 2021. Available from: https://ecampusontario.pressbooks.pub/remotesensing/.

Llano XC. SMByC-IDEAM AcATaMa - QGIS plugin for Accuracy Assessment of Thematic Maps, version 24.12c. smbyc.github. [Online].; 2024. Available from: https://smbyc.github.io/AcATaMa.

Olson CE. Is 80% Accuracy Good Enough? In Pecora 17 - The Future of Land Imaging; 2008; Denver, Colorado: Asprs.org.

Sari AN, Pranoto R, Suryan V. Perhitungan Hidrograf Banjir dengan Metode Hidrograf Satuan Sintesis SCS (Soil Conservation Service) di Kota Palembang. Journal of Airport Engineering Technology (JAET). 2020;: 1-7.

Siddique AR. Curve Number Generator: A QGIS Plugin to Generate Curve Number Layer from Land Use and Soil. Github. [Online].; 2020. Available from: https://github.com/ar-siddiqui/curve_number_generator.

Siddiqui AR. Area-Weighted-Average: Plugin to perform Area Weighted Average analysis in QGIS. Github.com. [Online].; 2021. Available from: https://github.com/ar-siddiqui/area_weighted_average.

Sitorus SRP, Leonataris C, Panuju DR. Analisis Pola Perubahan Penggunaan Lahan dan Perkembangan Wilayah di Kota Bekasi, Provinsi Jawa Barat. Jurnal Tanah Lingkungan. 2012;: 21-28.

Sunandar Y.). Mengenal Cekungan Bandung dan DAS Citarum. Walungan.org. [Online]. Bandung: Walungan.org; 2024. Available from: https://walungan.org/2024/01/31/mengenal-cekungan-bandung-dan-das-citarum/.

Tisnasuci ID, Sukmono A, Hadi F. Analisis Pengaruh Perubahan Tutupan Lahan Daerah Aliran Sungai Bodri terhadap Debit Puncak Menggunakan Metode Soil Conservation Service (SCS). Jurnal Geodesi Undip. 2021;: 105-114.

USACE. HEC-HMS Technical Reference Manual. hec.usace.army.mil. [Online].; 2025. Available from: https://www.hec.usace.army.mil/

USACE. HEC-RAS User's Manual. hec.usace.army.mil. [Online].; 2025. Available from: https://www.hec.usace.army.mil/confluence/rasdocs/rasum/latest.

Wulansari H. Uji Akurasi Klasifikasi Penggunaan Lahan dengan Menggunakan Metode Defuzzifikasi Maximum Likelihood Bebasis Citra ALOS-AVNIR-2. Bhumi. 2016;: 98-110.